Atmospheric Environment 198 (2019) 194–206

Contents lists available at ScienceDirect

Atmospheric Environment

journal homepage: www.elsevier.com/locate/atmosenv

The effects of simulating volcanic aerosol radiative feedbacks with WRF-Chem during the Eyjafjallajökull eruption, April and May 2010

Marcus Hirtl[a,b,*], Martin Stuefer[b], Delia Arnold[a,e], Georg Grell[c], Christian Maurer[a], Stefano Natali[d], Barbara Scherllin-Pirscher[a], Peter Webley[b]

[a] Section Chemical Weather Forecasts, ZAMG – Zentralanstalt für Meteorologie und Geodynamik, Vienna, Austria
[b] Geophysical Institute, University of Alaska Fairbanks, Fairbanks, AK, USA
[c] NOAA/ESRL/Global Systems Division, Boulder, CO, USA
[d] SISTEMA GmbH, Vienna, Austria
[e] Arnold Scientific Consulting, Manresa, Spain

ARTICLE INFO

Keywords:
Aerosol radiative feedback effects
WRF-Chem
Eyjafjallajökull eruption 2010
Volcanic ash plume
Model evaluation

ABSTRACT

Explosive volcanic eruptions can inject large amounts of ash and gases into the atmosphere. Such volcanic aerosols can have a significant impact on the surrounding environment, and there is the need to closely investigate their effects on meteorology on local, regional, and even continental scale. This work presents a study of the 2010 Eyjafjallajökull volcanic eruption the resulting ash dispersion and its radiative feedback effects on the meteorological conditions with the Weather Research Forecasting model with on-line Chemistry (WRF-Chem). Two model runs, one meteorology-only simulation (without chemistry) and one that considers gas- and aerosol chemistry as well as direct- and semidirect aerosol feedbacks were performed and compared. Results for daily values show that aerosol radiative feedback effects can cool the atmosphere close to the surface on average by 1 °C with maximum cooling exceeding even 2 °C for the considered episode. Near-surface atmospheric wind speed changed on average by 0.5 m/s with maximum values above 2 m/s. Furthermore, the presence of ash aerosols affected the vertical shape of the profiles of wind speed and temperature and resulted in a better agreement with radiosonde measurements when radiative feedback effects were considered. Although the modeling of the dispersion of volcanic ash clouds is subject to large uncertainties, we have demonstrated that the WRF-Chem model can reproduce observations at surface levels and vertical profiles more realistically when radiative feedback effects are considered in the simulations.

1. Introduction

Aerosols are known to have an impact on the weather and climate via their direct effect on radiation (Charlson et al., 1992; Jacobson et al., 2007; Thordarson and Self, 2003) and their impact on cloud formation (Twomey, 1977) and have been implemented into several numerical weather prediction (NWP) models (e.g., Grell et al., 2005; Solomos et al., 2011; Bangert et al., 2011). Furthermore, absorbing aerosols cause changes in surface temperature, wind speed, relative humidity, clouds, and atmospheric stability through the semi-direct effect (e.g., Hansen et al., 1997; Baró et al., 2017). In order to account for these effects, models are necessarily on-line coupled meteorology-chemistry models, which means that both the chemical and meteorological components are included in one single system. An overview of different integrated models developed and applied in the US and in Europe can be found in Zhang (2008) and Baklanov et al. (2014).

Within the phase 2 of the Air Quality Model Evaluation International Initiative (AQMEII http://aqmeii.jrc.ec.europa.eu/, Alapaty et al., 2012) eight different regional coupled chemistry and meteorology models were evaluated. Forkel et al. (2015) showed that the direct aerosol effect reduced the seasonal mean solar radiation by 20 Wm^{-2} and the seasonal mean temperature by 0.25 °C. The AQMEII-2 studies of Brunner et al. (2015) showed that different model systems generated greater differences than a single model system that includes or excludes aerosol feedback effects. The AQMEII-2 studies revealed (e.g. San José et al., 2015) that it is difficult to demonstrate positive impacts of aerosol-atmosphere feedback effects on NWP due to variations of the aerosol parameterization schemes within the different models, and due to the lack of significant aerosol concentrations during the chosen test periods. However, this conclusion may be different for

* Corresponding author. Section Chemical Weather Forecasts, ZAMG – Zentralanstalt für Meteorologie und Geodynamik, Vienna, Austria.
E-mail address: marcus.hirtl@zamg.ac.at (M. Hirtl).

https://doi.org/10.1016/j.atmosenv.2018.10.058
Received 19 May 2018; Received in revised form 7 October 2018; Accepted 28 October 2018
Available online 02 November 2018

episodes with high aerosol loads such as during the Russian forest fires 2010 (Kong et al., 2015). Grell et al. (2011) used the WRF-Chem model (Grell et al., 2005) to simulate the interaction of Alaska wildfire aerosols with atmospheric radiation and microphysics. Accounting for the aerosol feedback resulted in significant modifications of the vertical profiles of temperature and moisture in cloud-free areas. During daytime, a strong direct effect was apparent. Interaction of the aerosols with atmospheric radiation through scattering and absorption was also significant and resulted in cooler surface temperatures in cloud-free areas.

In this study we used the WRF-Chem model to investigate radiative feedback effects caused by volcanic ash clouds, on meteorology based on the already proven capability of WRF-Chem to realistically simulate emissions from volcanic eruptions (Stuefer et al., 2012). A volcanic source term parameterization provides us with the possibility to include time varying ash and sulfur dioxide emissions from volcanic eruptions. The volcanic module of WRF-Chem has been tested for several cases (i.e. Mount Redoubt, Alaska, 1989 and Eyjafjallajökull Volcano, Iceland, 2010) showing good agreement with observations such as infrared satellite data and ground-based lidar. Webley et al. (2012) provided a detailed evaluation of the eruption of Eyjafjallajökull in Iceland in 2010 and demonstrated that the proper knowledge of model input parameters, such as volcanic plume height, mass eruption rate, particle size distribution and duration, are essential to realistically forecast ash concentrations.

In this study the influence of radiative feedback effects on wind speed and temperature is investigated during the eruption of Eyjafjallajökull volcano, Iceland, in April and May 2010. The description of the volcanic eruption, the WRF-Chem model configuration and the scenarios setup are described in Sections 2. In Section 3, the simulated temporal- and spatial distribution of the ash plume is evaluated with satellite, PM10, and LIDAR observations. The description of meteorological measurements and a general model evaluation for the whole considered period and all stations is summarized in Section 4. The effects of aerosol feedbacks on the model performance are investigated in Section 5. The impact of considering feedback effects on the dispersion of the plume is demonstrated in chapter 6 and concluding remarks are given in Section 7.

2. Simulations setup

2.1. Model setup and case specifications

The on-line coupled WRF-Chem model (v3.4) was applied for a domain extending over Europe, northern Africa, and Western Russia. Simulations were performed with a horizontal resolution of 12 km. Analysis and forecast data (resolutions – (1) horizontal: 0.25°, (2) vertical: 91 model levels, and (3) temporal: 3 hourly) provided by the global Integrated Forecast System (IFS) model operated at the European Centre for Medium-Range Weather Forecast (ECMWF) were used to initialize the model.

In order to investigate the impact of aerosol feedback effects on meteorology, two WRF-Chem simulations were performed and compared. The first run, the reference or base case scenario, considers only meteorology without any chemistry ('onlyMET'). The onlyMET run also considers aerosols, but only uses an aerosol climatology with no information on the volcanic eruption. The second 'VOLC' scenario considers gas-phase- and aerosol-chemistry using anthropogenic, biogenic-, and natural emissions. The following physics options were applied for both simulations: Rapid Radiative Transfer Method for Global (RRTMG) long-wave and short-wave radiation scheme (Iacono et al., 2008), Yonsei University (YSU) Planet Boundary Layer (PBL) scheme (Hong et al., 2006), NOAH land surface model (Chen and Dudhia, 2011), and the Grell three-dimensional (3D) ensemble cumulus parameterization (Grell and Freitas, 2013) with radiative feedback.

To consider the aerosol direct effect, aerosol optical properties (extinction coefficients, single scattering albedo, and asymmetry factor) are calculated as a function of wavelength and position (3D), and then transferred to the radiation scheme. For the used aerosol option MADE/SORGAM, the finest three ash bins – depending on their size – are added to the respective PM10 and PM2.5 variables, which are defined as unspeciated aerosols which enables the capability to include volcanic aerosol interaction with radiation (shortwave as well as long wave) and cloud microphysics (not used in this study).

The VOLC run was based on the Regional Acid Deposition Model (RADM2) module (Stockwell et al., 1990) for the gas-phase chemistry as well as the Modal Aerosol Dynamics Model for Europe (MADE)/Secondary Organic Aerosol Model (SORGAM) module to describe the aerosol chemistry (Ackermann et al., 1998; Schell et al., 2001). No aqueous phase chemistry was considered (WRF-Chem chem_opt = 2 was used without aerosol indirect effects). To provide realistic chemical initial conditions, a 9-day spin-up period (5 April to 13 April 2010) was applied.

A 40-day period from April 14 until May 23, 2010, was simulated with WRF-Chem as a sequence of two-day time slices. The initial chemical state at the beginning of each time slice was adopted from the final state of the previous time slice, while meteorology was re-initialized with ECMWF analysis every second day using a 12-h meteorological spin-up. An implicit inclusion of aerosol impacts in these input fields (e.g. through data assimilation of wind and temperature in the ECMWF model) is considered very small as the input fields are much coarser than the WRF-Chem simulations which have their own dynamics.

Anthropogenic emissions were obtained from the Netherlands Organization for Applied Scientific Research inventory (TNO, Visschedijk et al., 2007). In addition, anthropogenic emissions from the European Monitoring and Evaluation Program (EMEP) inventory (e.g., Vestreng et al., 2006, http://www. ceip.at/ceip) were included for areas not covered by TNO. These areas are located mainly in Africa and Asia. The simulations also considered biogenic emissions (Guenther, 2006) as well as dust and sea salt emissions.

2.2. Volcanic emission preprocessor

The Eruption Source Parameters (ESP) for the Eyjafjallajökull eruptive event were provided by Mastin et al. (2014). We used 3-hourly plume heights and respective emission rates of ash. The plume height information was provided by a combination of data from a C-band Doppler radar system and a multiple web camera imagery (Arason et al., 2011). The emission rates were derived empirically using the observed plume heights (Mastin et al., 2009). The time series of the 3-hourly emitted ash mass was further scaled with the total erupted mass as provided by Gudmundsson et al. (2012), who estimated total emissions for the different phases of the Eyjafjallajökull eruption lasting from April 14, 2010, until May 18, 2010. A total emission of 170 Tg and 190 Tg were estimated for phase I (14–18 April) and for phase III (4–18 May), respectively. During phase II (19 April – 3 May) only low discharge diffusion was observed. Fig. 1 summarizes the emission heights and rates used in the WRF-Chem model initialization.

The pre-processor for volcanic emissions used in this study is based on a modified emission pre-processor from Freitas et al. (2011) that uses the time series of volcanic source data (emitted mass and plume height) as in Fig. 1. The volcanic ash and sulfur dioxide (SO_2) plumes are vertically distributed to an umbrella shape with 75% of the erupted mass in the area surrounding the specified top plume height (parabolic distribution, Fig. 2) and 25% of the mass linearly distributed underneath.

The model considers ash particles smaller than 63 μm (fine ash) distributed over 10 particle size bins to better predict ash fall as well as atmospheric transport in relation to the different sizes (Stuefer et al., 2012). The distribution of the volcanic ash into the model bins is based on historic volcanic eruptions and depends on the eruption type. In this

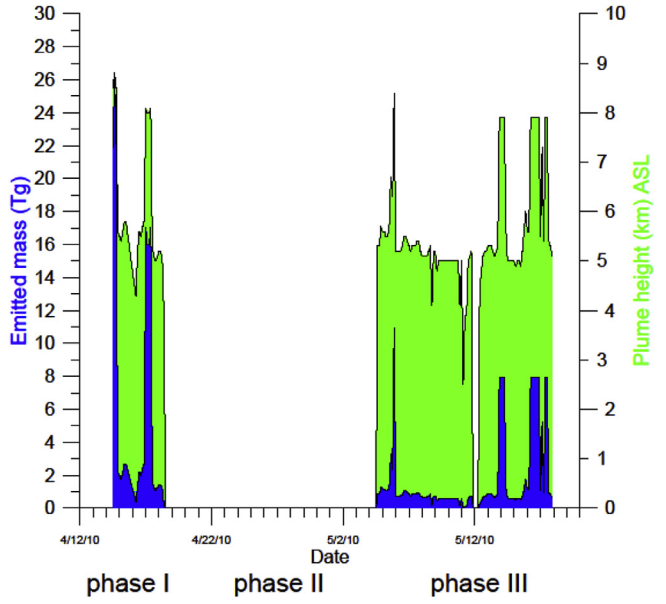

Fig. 1. Estimated plume heights (green, 3-hourly) and derived emitted mass (blue) used in the WRF-Chem modeling simulations (VOLC) for the eruption period April 14 until May 18, 2010. (For interpretation of the references to colour in this figure legend, the reader is referred to the Web version of this article.)

work, the option that allows to add the ash to the PM2.5 and PM10 particle variables within WRF-Chem was used. This approach enables the inclusion of volcanic aerosol interaction with radiation and cloud microphysics.

The total ash mass is distributed between 10 bins of aerosol particles with diameter size ranging between 2 mm and less than 3.9 µm. For this study the classification S2 (see Table 1) was used according to Stuefer et al. (2012).

Table 1
Ash particle bin size ranges with corresponding WRF-Chem bins (1–10); the mass fractions in percent of total mass are given in the 3rd column for the used classification S2.

bin	Particle size diameter	S2
1	1–2 mm	22.0
2	0.5–1 mm	5.0
3	0.25–0.5 mm	4.0
4	125–250 µm	5.0
5	62.5–125 µm	24.5
6	31.25–62.5 µm	12.0
7	15.625–31.25 µm	11.0
8	7.8125–15.625 µm	8.0
9	3.9065–7.8125 µm	5.0
10	< 3.9 µm	3.5

The simulated ash plume is highly sensitive to the eruption source parameters (ESP). Initial simulations of the Eyjafjallajökull case revealed that the representation of the source geometry had to be adjusted for this particular case. Since the mass distributed to the lower atmospheric levels was strongly overestimated, two changes were implemented within the volcanic WRF-Chem parameterization (see also Fig. 2):

1.) A large difference between model vent height and real height of the Eyjafjallajökull was found. Due to the smoothed model topography (with the horizontal resolution of 12 km) the top height of the volcano was at 600 m above sea level (ASL), while the real vent height is about 1000 m higher at 1600 m ASL. The code was adjusted to consider the vent height as an additional parameter to avoid atmospheric dispersion of volcanic ash at altitudes below the real vent height.
2.) The default vertical plume shape assumes a 75:25 (umbrella:linear-part) distribution of the mass emissions, which seems to be

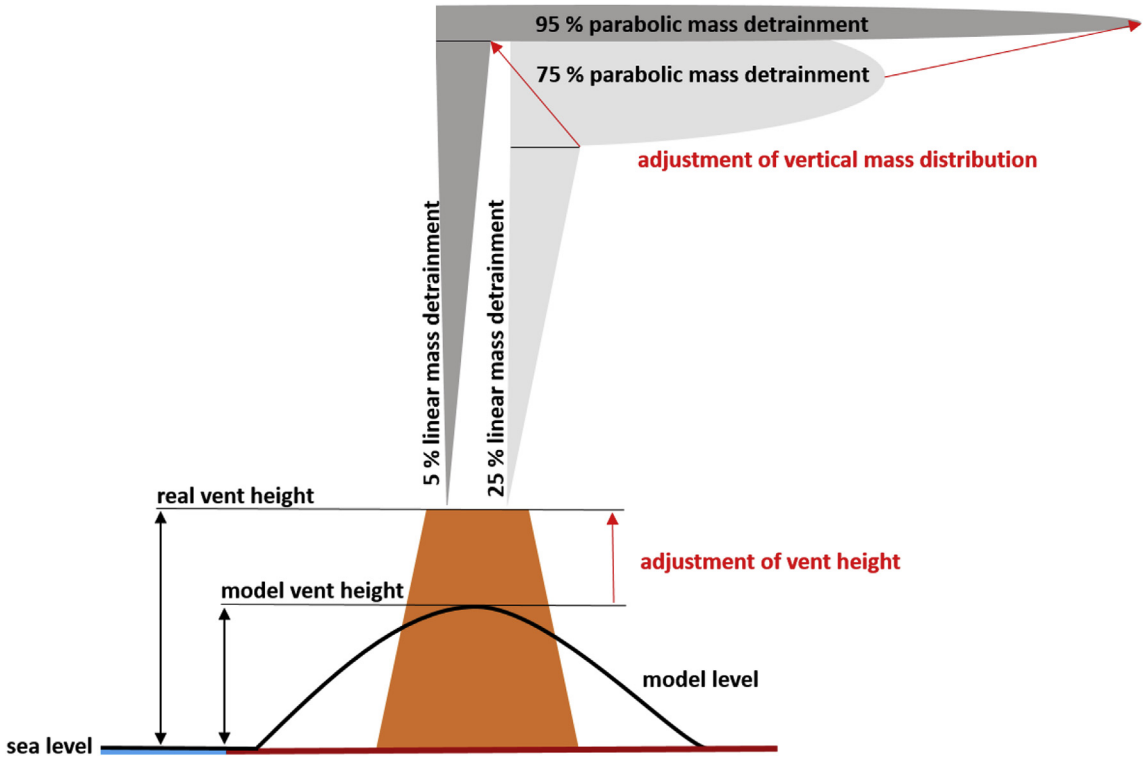

Fig. 2. *Exemplified ash plume representation with the adjustments conducted for WRF-Chem, with the original 75% parabolic mass detrainment and volcano summit as depicted in the* 12 km *grid.* Adjustment to 95% for the parabolic mass detrainment for explosive phases and the correct vent height was used in this study.

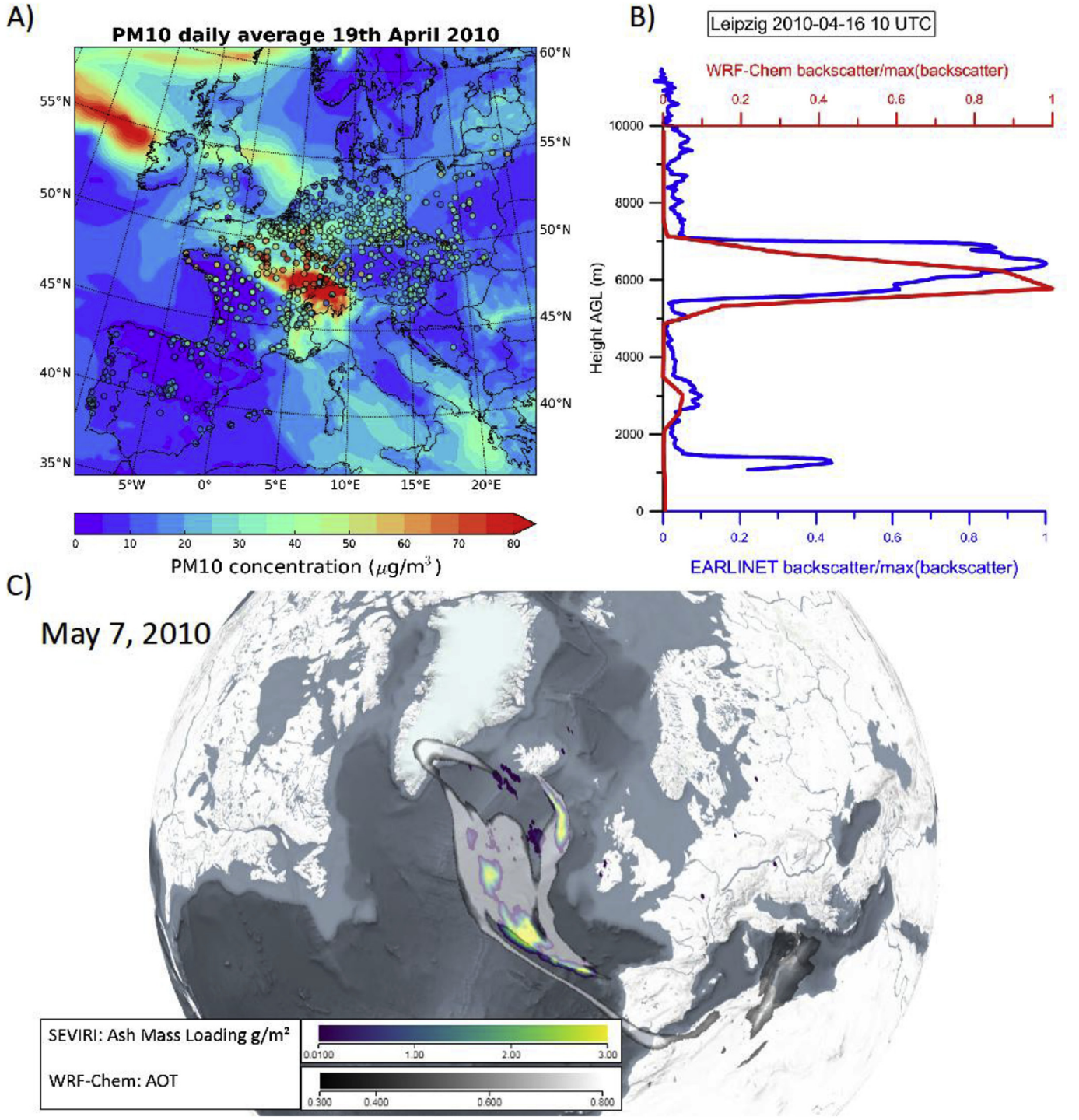

Fig. 3. Comparison of the WRF-Chem simulation with (A) observations of daily average PM10 ground concentrations, (B) vertical profiles of normalized backscatter coefficients from EARLINET, and (C) SEVIRI ash mass loading.

inaccurate during the times of explosive eruptions. In our simulations we have assumed that during timesteps when a strong increase of plume height occurs the mass is shifted to higher altitudes. We account for that fact by allocating only 5% of the mass to the linear part of the initial plume and 95% of the mass to the umbrella shape at the top of the plume. This 95:5 distribution was used during the times when the plume heights were raised above 8000 m ASL. For all other times the proposed, and WRF-Chem model default, standard distribution 75:25 was used.

3. Spatial and temporal evaluation of the location of the volcanic plume

To evaluate the temporal and spatial location of the simulated volcanic ash cloud of the Eyjafjallajökull eruption, WRF-Chem model simulations were compared to observations. As the focus of this paper is on the evaluation of meteorological parameters with respect to feedback effects, only a sub-set of relevant results are shown (Fig. 3).

European-wide ground measurements from EEA (European Environmental Agency) were used to evaluate the simulated PM10

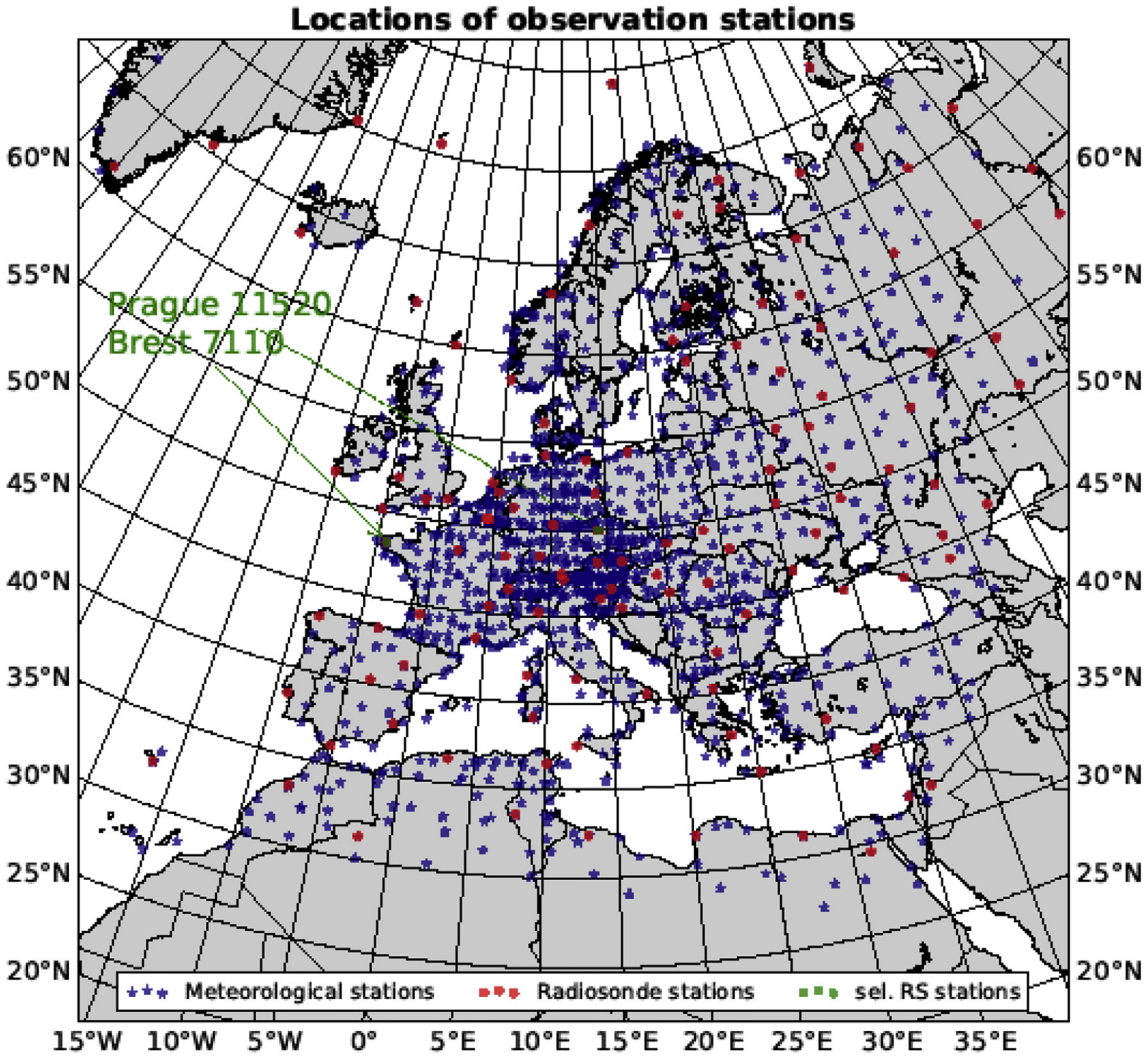

Fig. 4. Locations of meteorological ground stations (blue) and radiosonde (red and green) observations used to be compared with the WRF-Chem modeling simulations in this study. (For interpretation of the references to colour in this figure legend, the reader is referred to the Web version of this article.)

Table 2
Statistics for the whole period (April 14 until May 23, 2010) and all measurement stations for 10 m wind speed, WS10, (left) and 2 m temperature, T2, (right).

WS10	*onlyMET*	*VOLC*	*OBS*	*T2*	*onlyMET*	*VOLC*	*OBS*
MEAN (m/s)	4.60	4.60	3.36	MEAN (°C)	7.35	7.30	9.50
SDEV (m/s)	2.61	2.61	2.54	SDEV (°C)	5.60	5.58	5.66
CORR	0.44	0.44		CORR	0.72	0.72	
FBIAS	0.31	0.31		FBIAS	−0.25	−0.26	
NMSE	0.57	0.57		*NMSE*	0.31	0.32	
NUM	*344065*			*NUM*	*345713*		

Table 3
Statistics at Brest from 16 to 18 April 2018 for 10 m wind speed, WS10, (left) and 2 m temperature, T2, (right). Only daytime measurements are considered.

WS10	*onlyMET*	*VOLC*	*OBS*	*T2*	*onlyMET*	*VOLC*	*OBS*
MEAN (m/s)	*5.10*	*5.11*	*5.27*	MEAN (°C)	*14.05*	*13.66*	*13.43*
SDEV (m/s)	*2.14*	*2.01*	*2.28*	SDEV (°C)	*2.75*	*2.85*	*2.94*
CORR	*0.80*	*0.81*		CORR	*0.92*	*0.92*	
FBIAS	*−0.033*	*−0.032*		FBIAS	*0.045*	*0.017*	
NMSE	*0.067*	*0.064*		*NMSE*	*0.008*	*0.007*	
NUM	*12*			*NUM*	*12*		

concentrations for those days when the dispersing ash cloud was close to the surface. In central Europe, peak PM10 concentrations were observed in April only a few days after the first eruption. Fig. 3A shows the PM10 ground concentrations (daily average - coloured circles) compared to the modeled concentrations on April 19. The simulated cloud was located over France and southern Germany and Switzerland. The observed peak-concentrations are reproduced by the model near the borders of France, Switzerland, and Germany. Schaefer et al. (2011) showed similar results for Germany. The comparison with ground PM10 measurements also for other days (not depicted) reveals that the parameterization of the source strength and geometry of the initial plume produced quantitative and qualitative realistic aerosol distributions.

The vertical location of the plume was evaluated with data from the European Aerosol Research Lidar Network (EARLINET), which provides long-term multi-wavelength backscatter and extinction coefficient profiles. The vertical backscatter coefficient profile of the VOLC WRF-Chem run is compared to the EARLINET measurement at Leipzig (Fig. 3B). The profiles are normalized with the maximum values so that the scale ranges from 0 to 1. The peak of the normalized backscatter coefficient between 5 km and 7 km is caused by the volcanic ash cloud. The simulation agrees well with the observation at this particular location and time. This means that WRF-Chem is able to represent the vertical location of the ash cloud keeping in mind the uncertainties that

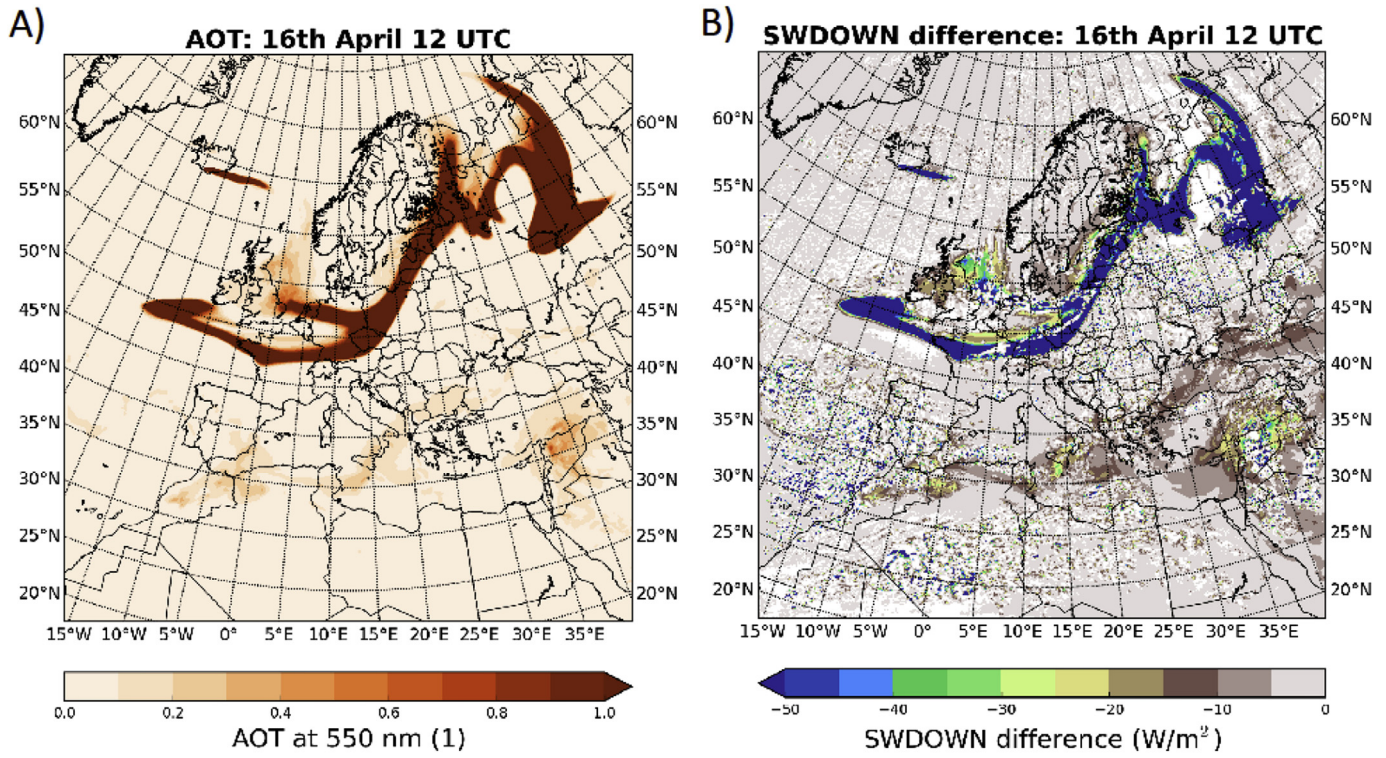

Fig. 5. 16 April 2010, 12 UTC. Left: AOT calculated from the VOLC run. Right: Short wave downward radiation flux (SWDOWN) difference between VOLC and onlyMET.

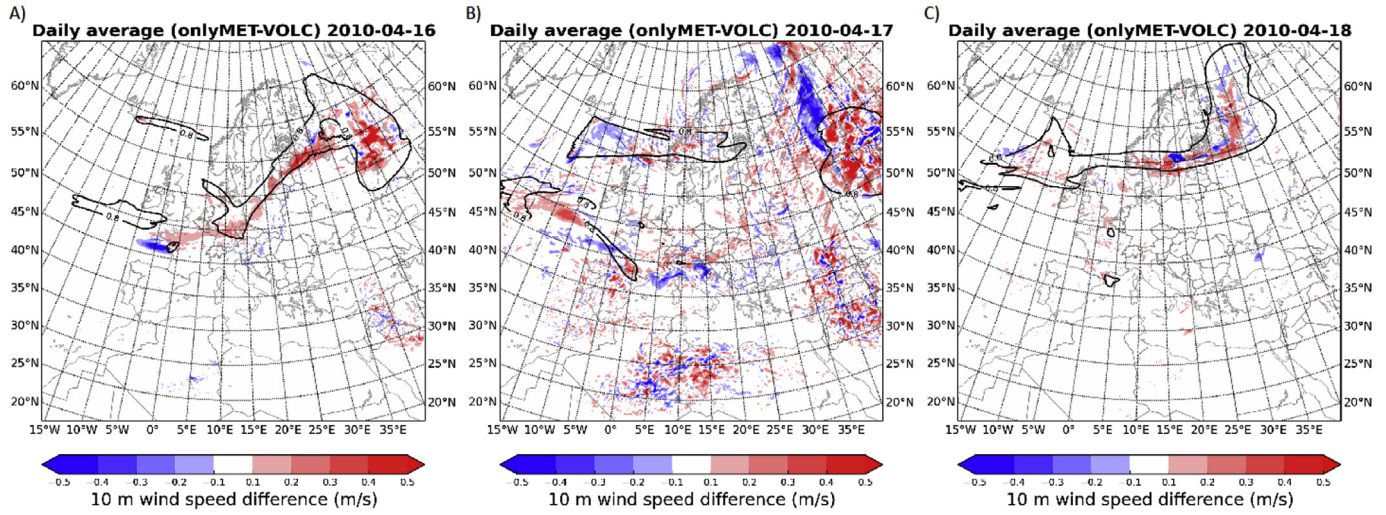

Fig. 6. Difference of daily average 10 m wind speed distribution between the two model runs (onlyMET-VOLC) for selected days in April 2010. Black: 0.8 AOT contour line.

are related to the representation of the volcanic emission source and especially its initial vertical distribution. The observed elevated aerosol distribution in the lower levels of the atmosphere represents accumulated aerosols in the boundary layer, which in this case are not resolved by the model.

Data from SEVIRI (Spin Enhanced Visible and Infra-Red Instrument) was used to qualitatively evaluate the regional extent and location of the volcanic plume (Fig. 3C). We compared WRF-Chem-derived atmospheric optical thickness (AOT) with the total ash load observed by the SEVIRI instrument for a selected day in May. A very good coincidence between model and observation is demonstrated for the cloud location in the vicinity (south-east) of the volcano.

4. Evaluation of meteorological parameters close to the surface

4.1. Meteorological observations

Evaluation of the WRF-Chem runs was performed with 2 m temperature and 10 m wind speed data from more than 1500 meteorological ground stations. In addition, daily observations at 00 UTC and 12 UTC from radiosonde data from the European network (Fig. 4) were used for the comparison with model-based vertical profiles of temperature and wind speed.

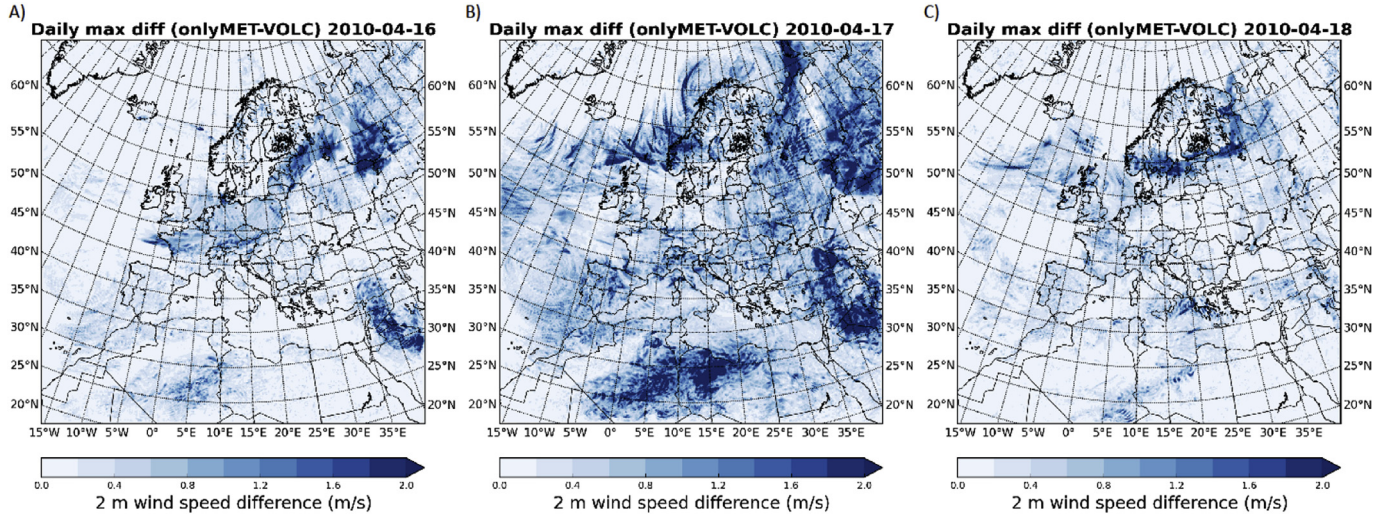

Fig. 7. Daily absolute maximum differences of the 10 m wind speed distribution for selected days in April 2010.

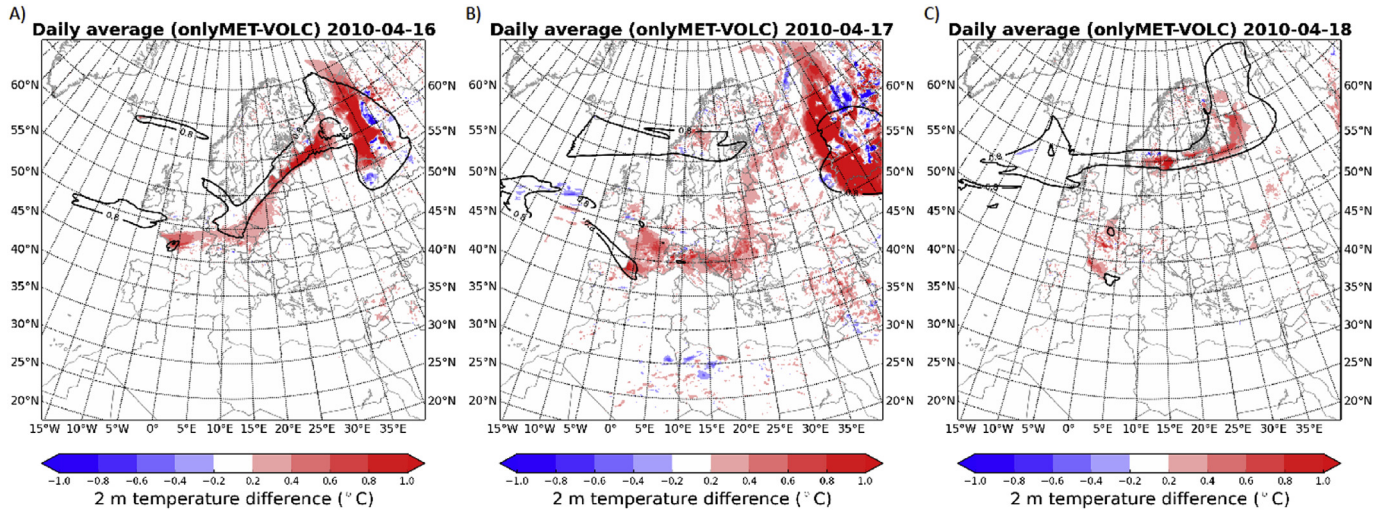

Fig. 8. Difference of the daily average 2 m temperature distribution between the two model runs (onlyMET-VOLC) for selected days in April 2010. Black: 0.8 AOT contour line.

Table 4
Statistics at all stations from 16 to 18 April 2018 for 10 m wind speed, WS10, (left) and 2 m temperature, T2, (right). Only daytime measurements are considered.

WS10	*onlyMET*	*VOLC*	*OBS*	*T2*	*onlyMET*	*VOLC*	*OBS*
MEAN (m/s)	*4.22*	*4.09*	*2.90*	MEAN (°C)	*10.12*	*9.9*	*7.5*
SDEV (m/s)	*2.08*	*2.07*	*1.15*	SDEV (°C)	*6.21*	*6.22*	*7.06*
CORR	*0.90*	*0.90*		CORR	*0.90*	*0.90*	
FBIAS	*0.37*	*0.34*		FBIAS	*2.29*	*0.27*	
NMSE	*0.24*	*0.22*		*NMSE*	*0.211*	*0.203*	
NUM	*3578*			*NUM*	*3596*		

4.2. Average meteorological parameters at ground level

Quantitative evaluation of the entire period of the eruption, from April to May 2010, was performed for both model runs with the observational data. The statistical indices comprise mean values (MEAN), standard deviation (SDEV), correlation coefficient (CORR), fractional bias (FBIAS), and normalized mean square error (NMSE). The number of considered data pairs (number of stations and time steps - NUM) is also indicated. It should be noted that the modeled gridded values were compared to point measurements and systematic differences can occur especially when stations are located in regions where the model resolution cannot represent sub-grid scale processes (e.g., Zhang et al., 2015).

Table 2 reveals that both wind and temperature have a fractional bias compared to the observations. Simulated mean wind is over-estimated by about 1.2 m/s while average temperature is under-estimated by more than 2 °C. However, correlation between model results and observations is higher for temperature (r = 0.72) than for wind speed (r = 0.44). Also, the NMSE is worse for wind speed and almost twice as high (0.57) than for the temperature (0.31 for onlyMET).

Similar results were found by Zhang et al. (2009) and Brunner et al. (2015), using WRF-Chem simulations with comparable horizontal resolutions. Other studies found improved results using significantly higher-resolved model simulations of 3 km (Zhang et al. (2015) using WRF-Chem, Seity et al. (2011) using the models ALADIN and AROME).

5. Aerosol radiative feedback effects in the model simulations

5.1. Radiative feedback effects close to the surface

The analysis in the previous section showed that the differences between the two model runs are negligible when the whole simulation period of 40 days is evaluated. This is due to the large number of

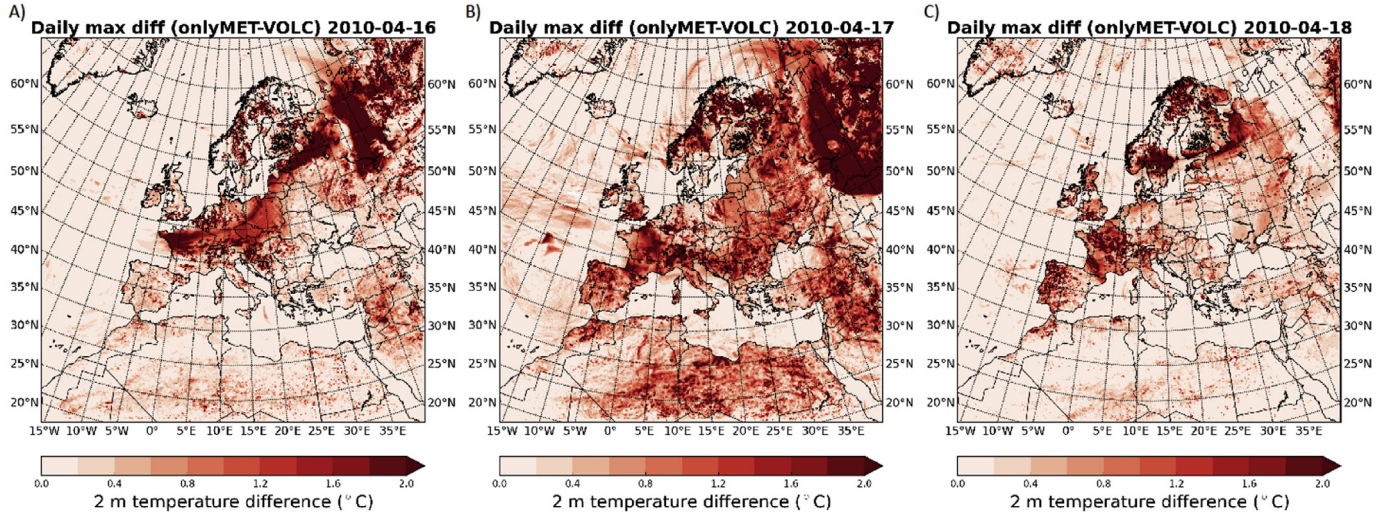

Fig. 9. Daily absolute maximum differences of the 2 m temperature distribution for selected days in April 2010.

stations that are not located near the ash cloud. Furthermore, periods during nighttime (without incoming solar radiation) were included in this comparison, which mask radiative feedback effects. To better quantify radiative feedback effects caused by the volcanic ash cloud during daytime, a statistical comparison was performed for a selected station in France (Brest, see Fig. 4) for the period from 16 to 18 April (Table 3). This station was selected because the volcanic ash cloud was passing by the station during these days (see Figs. 6 and 8). Statistical measures given in Table 3 were obtained only from daytime measurements (9/12/15/18 UTC).

Table 3 reveals reduced biases and a better agreement to observations when considering radiative feedback effects from atmospheric aerosols. While improvements in terms of 10 m wind speed are small (the mean value reduces only by 0.1 m/s), the 2 m temperature mean value decreases significantly by 0.39 °C and results in differences to only about 0.2 °C for the VOLC run to the observations. The FBIAS, CORR and the NSME are also slightly better for the VOLC run.

This analysis can also be expanded to the other stations. For these 3 days the analysis is also done for the other stations (see Table 4) applying the same filtering as for the results obtained in Table 3. A similar effect can be observed as for the single station, in this example wind speed and temperature are decreased in the VOLC run and fit better to the measurements in the example.

The differences in wind speed and temperature are an effect of reduced incoming radiation caused by the presence of the volcanic ash cloud. The effect is shown in Fig. 5 which depicts the location of the ash cloud (Fig. 5A) and the resulting difference between the two model runs (onlyMET-VOLC) in the short-wave downward radiation flux (Fig. 5B). Negative values shown in Fig. 5B indicate regions that receive less incoming short-wave radiation due to aerosol layers aloft. The highest differences in radiation have values greater than 50 W/m^2.

The differences of near-surface winds and temperatures on a daily basis (average and maximum values) between the VOLC- and the onlyMET (DIFF = onlyMET-VOLC) runs are shown for three consecutive days during the first phase of the eruption in Figs. 6–9. During these days (April 16 to April 18, 2010), highest ash loads were observed over Europe. To facilitate the interpretation of the model runs, the location of the volcanic ash cloud is indicated by the daily average 0.8-AOT contour-line from the VOLC run.

The differences between the daily average 10 m wind speed of the two model runs (Fig. 6) can be both negative and positive and range within ± 0.5 m/s. The maximum magnitudes of the wind speed differences are co-located with the ash cloud. Since the model simulations were performed as sequences of two-day time slices with meteorological conditions initialized every other day, feedback effects are stronger and wider-spread on the second day of the simulation (i.e., on April 17) than on the first day (April 16 and April 18).

The maximum daily difference of the wind speed between the two model runs (Fig. 7) exceeds 2 m/s in some regions. Note, that radiative feedback effects far away from the volcanic ash cloud (e.g., wind speed differences in Northern Africa on April 17), are caused by local Saharan dust rather than the volcanic ash plume. This is because the VOLC run does not only include atmospheric aerosols from the volcanic eruption but also from other sources such as desert dust or anthropogenic emissions.

The presence of the volcanic ash cloud in the VOLC run lowers the incoming radiation at the surface, and therefore lower temperatures prevail compared to the onlyMET run. The daily average temperature differences are therefore positive reaching up to 1 °C (Fig. 8). Nevertheless, for some grid points the VOLC run even produces higher daily average temperatures, which can occur due to the influence of different air flow dynamics in the two runs. The daily maximum absolute differences of near-surface temperature are shown in Fig. 9. The highest differences occur over mainland and exceed 2 °C.

As already found for wind speed, the temperature differences of the two model runs increase with forecast time and are more pronounced on the 2nd day (April 17) of the simulations.

5.2. *Vertical profiles of wind speed and temperature*

Mean vertical profiles of wind speed and temperature are evaluated against radiosonde measurements at various locations for the whole period from April 14 until May 23, 2010. It should be noted that the lowest depicted levels of wind speed and temperature represent the lowest level rather than the surface.

Average wind speed profiles (Fig. 10A) of the two model runs agree to within ± 0.3 m/s. Compared to the observations, the average wind speed shows better agreement at upper levels/altitudes, but the model overestimates wind speeds at lower levels by up to 2 m/s (Fig. 10C). Slightly better agreement is found at the lowest levels, where the average model wind speed is larger than that of the observations by only 0.8 m/s, which confirms results of the surface parameters (see Table 2).

In analogy, Fig. 10B shows the average temperature profiles at all levels/altitudes. At high altitudes (above 300 hPa), the average temperature simulated with the VOLC run is larger than that of the onlyMET run by up to 0.6 °C. At altitudes below 900 hPa, the two model runs differ by up to 0.4 °C with higher temperatures found for the

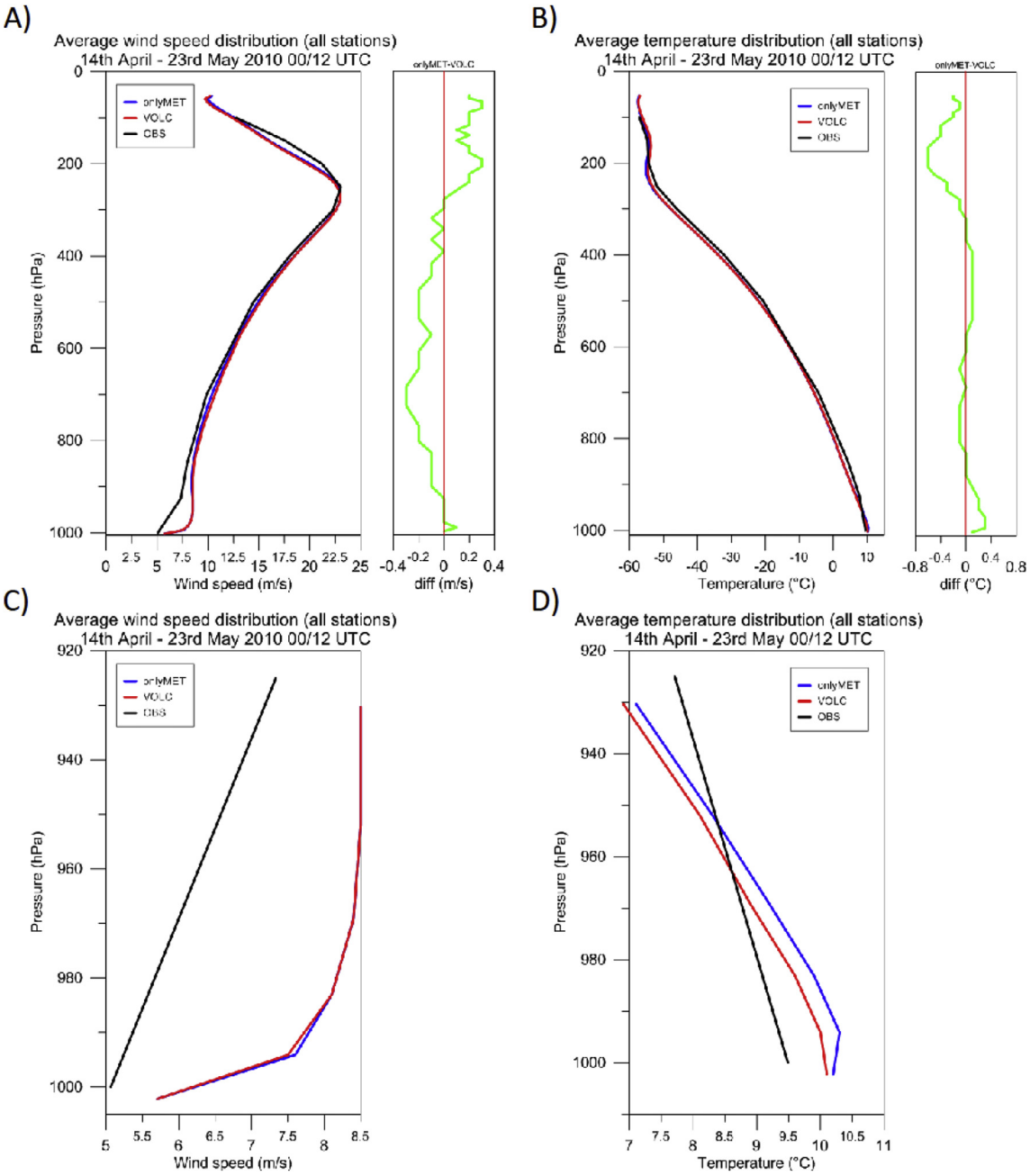

Fig. 10. Average vertical profiles of wind speed (A) and temperature (B) for all 122 radiosonde locations for 40 days compared to the model runs. C and D focus in on lower altitudes (> 920 hPa), within the WRF-Chem model.

onlyMET run. At these lower levels, simulations and observations agree to within 1 °C on average (Fig. 10D) showing better agreement of the VOLC run at altitudes below 960 hPa.

The vertical structure of the temperature distribution defines the height of the tropopause. This location of the tropopause is sensitive to temperature changes in the troposphere and stratosphere which has already been investigated in various studies (e.g. Reid and Gage, 1985; Santer et al., 2003a; Randel et al., 2000). Santer et al. (2003b) showed that volcanic aerosols during massive eruptions can also lower the tropopause because of the absorbed incoming solar radiation. This effect can also be found in the temperature distribution of the two model runs Fig. 10B. As the temperature is slightly higher in the VOLC run at the upper levels the simulated tropopause is slightly lower than in the onlyMET run.

5.3. Influence of the radiative feedback effects on the atmospheric stability

To investigate temperature differences between the two model runs at lower altitudes in more detail, individual profiles are investigated in this section.

An interesting situation happened on April 16 at the French station Brest (7110 in Fig. 11A), where the VOLC run simulated a temperature inversion slightly above 800 hPa that was also found in radiosonde measurements. The same effect, but a little weaker, was also found at other locations, e.g., in Prague (11520 in Fig. 11B).

The volcanic ash cloud reduces the incoming short-wave radiation at the surface, which leads to an improved thermal structure of the boundary layer and prevents the inversion to disappear during the morning hours.

The temporal evolution of the thermal structure of the boundary

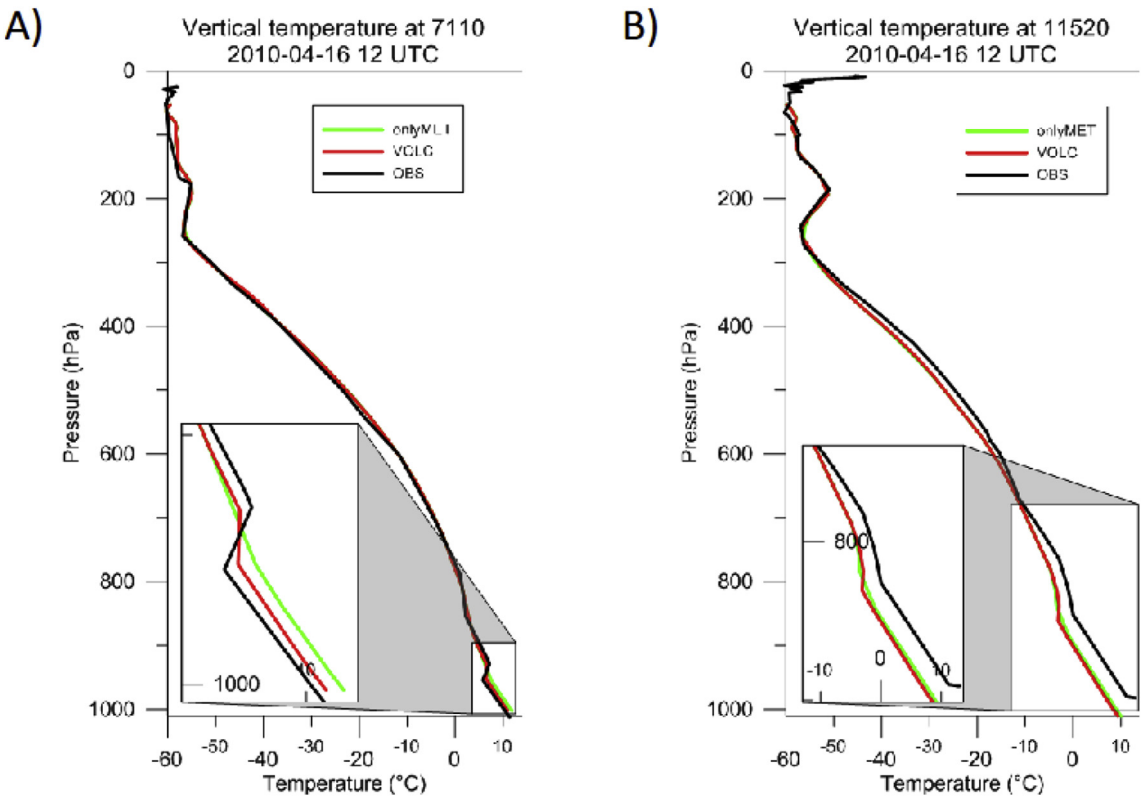

Fig. 11. Temperature profiles for the onlyMET and VOLC WRF-Chem runs at Brest (A, stat nr. 7110) and Prague (B, stat nr. 11520) compared to radiosonde measurements on 16 April 2010.

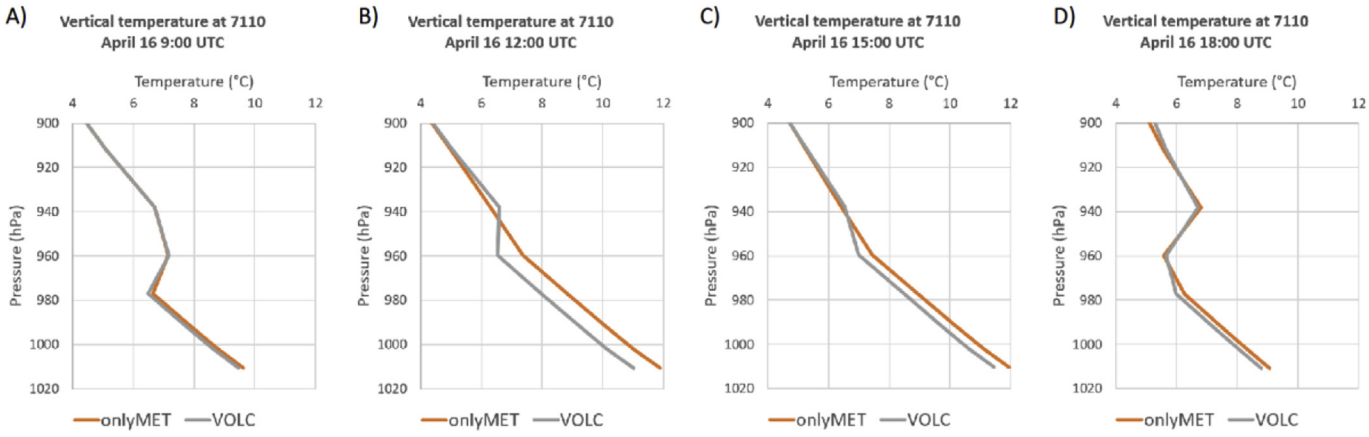

Fig. 12. Temporal evolution of the vertical temperature profile for the onlyMET (green) and the VOLC (red) run for April 16 at the station 7110 for (A) 9:00, (B) 12:00, (C) 15:00 and (D) 18:00 UTC. (For interpretation of the references to colour in this figure legend, the reader is referred to the Web version of this article.)

layer at Brest is illustrated in Fig. 12 that shows temperature profiles for different time steps on April 16, 2010. While at 09:00 UTC the inversion at 900 hPa is present in both model runs, it has almost disappeared in the onlyMET run at 12:00 UTC. The VOLC run, however, persistently keeps showing the inversion as do the radiosonde observations (see Fig. 11A). At the next time step, at 15:00 UTC, neither the VOLC run nor the onlyMET profile reveal a temperature inversion, which is established again in both simulations in the evening at 18:00 UTC.

6. The influence of considering the direct effect on the dispersion of the ash cloud

In the previous chapters we have shown that the wind distribution is altered at the surface and in vertical levels when direct aerosol effects are considered in the simulations. If the wind distribution is changed also the dispersion of the ash cloud is changed. To show this effect also a five-day simulation (forecast) was conducted without re-initialization of the meteorology. The results are depicted in Fig. 13, for 15 to 18 April at 12 UTC. Both model runs consider volcanic ash emissions, but only one run (green) uses direct feedback effects. It can be observed that as the forecasting period gets longer the fields deviate more and more as the time evolves. During the last 2 days of the forecast (Fig. 13C and D) already significant differences in the ash location can be found in some regions. This is relevant if dispersion models are used for emergency response during hazard situations.

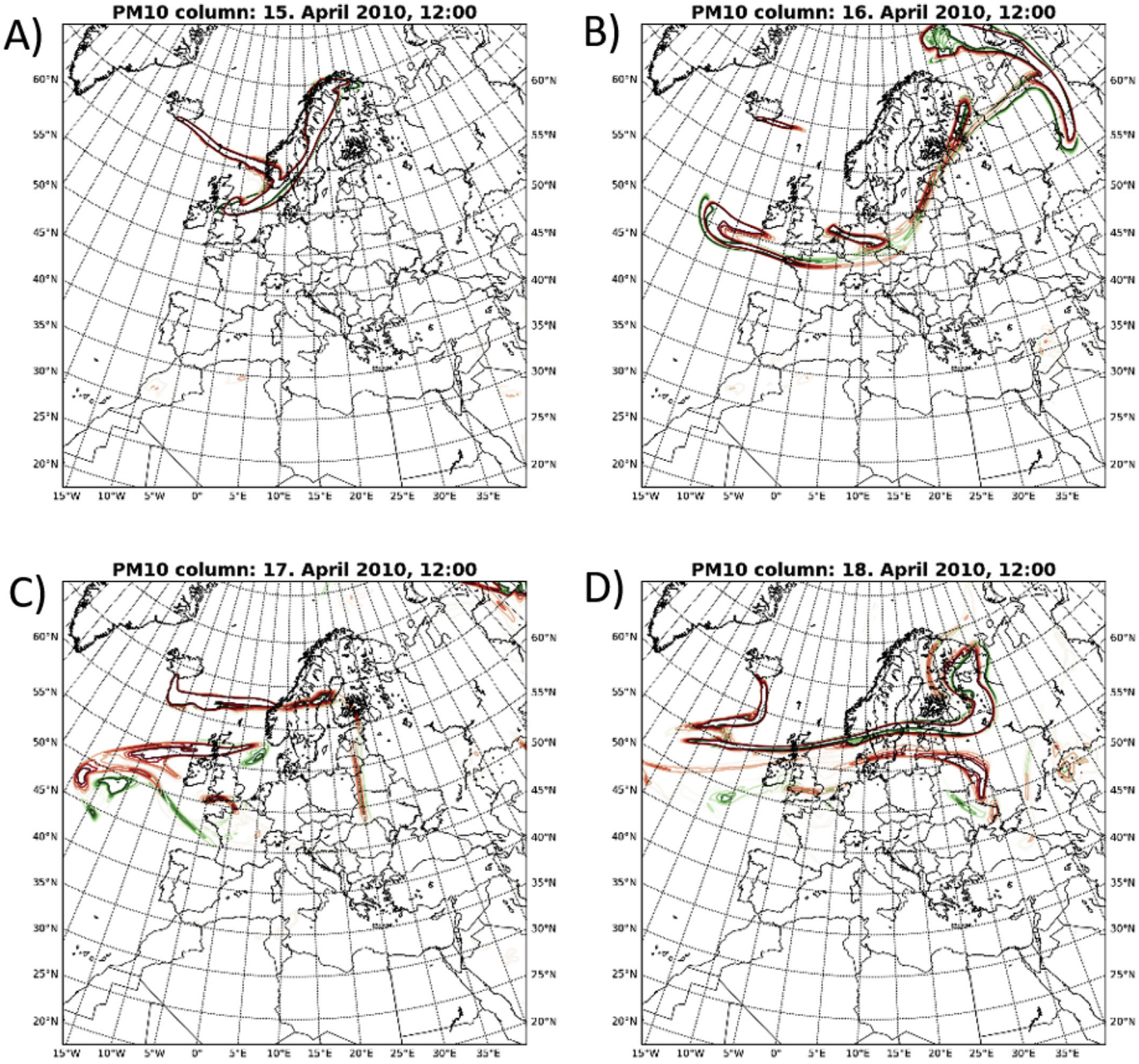

Fig. 13. Total PM10 columns for the simulations with (green) and without (red) radiative feedback turned on from 15th to 18th April 2010. (For interpretation of the references to colour in this figure legend, the reader is referred to the Web version of this article.)

7. Summary and conclusions

The dispersion of aerosols is strongly influenced by atmospheric conditions as described by the 4-D (x, y, z, and t) wind and temperature (stability) distribution. On the other hand, meteorological parameters can be changed due to the presence of aerosols in the atmosphere. The downward short-wave radiation flux is reduced through aerosols causing changes of standard atmospheric characteristics. In this study we evaluated a widely used aerosol feedback parameterization implemented in WRF-Chem. One goal of the experiments was to better understand the direct radiative feedback effects on temperatures and wind speeds at the near-surface as well as within the lower troposphere. Former studies, e.g., from Brunner et al. (2015), San José et al. (2015), and Forkel et al. (2015), revealed that further research is needed for heavy dust load events to better understand changes in meteorological parameters when feedback effects are considered. The WRF-Chem model was used in our study to simulate the dispersion of the volcanic ash cloud during the Eyjafjallajökull volcanic eruption in 2010. The model allowed us to investigate the influence of aerosol radiative feedback effects on the local, regional, and continental scale.

A series of major eruptions of the Eyjafjallajökull volcano in Iceland started on April 14, 2010 and continued until May 18, 2010. During that episode, the volcanic ash cloud dispersed over Europe. Two WRF-Chem simulation scenarios were conducted for the entire period of 40 days. An 'onlyMET' simulation using only meteorology without any chemistry and no aerosol-radiation feedback effects provided the base case scenario that was compared to the results obtained from a 'VOLC' model run considering gas- and aerosol chemistry as well as direct- and semi-direct aerosol feedbacks.

The temporal and spatial location of the modeled volcanic ash cloud agreed well with satellite data from SEVIRI. Vertical profiles of simulated extinction coefficients were also in good agreement with data

from the EARLINET lidar network. The comparison of simulated PM10 and ground-based PM10 measurements also confirmed that the parameterization of the volcanic emissions produced quantitative and qualitative realistic aerosol distributions.

Evaluation of the WRF-Chem model results with ground-based observations revealed a near-surface model bias of about +1.2 m/s in wind speed and −2.0 °C in temperature. Radiative feedback effects were negligible when averaging over the entire time period of 40 days.

Comparison of the two model runs showed that radiative feedback effects are largest below or close to the volcanic ash cloud. Differences between the model runs for the daily average wind speed can reach up to ± 0.5 m/s near the surface. The maximum daily wind speed difference can even exceed 2 m/s in some regions. While daily average temperature differences mainly remained within 1 °C, daily maximum differences at ground level were as large as 2 °C. Since the WRF-Chem experiment was designed to be re-initialized every other day, larger differences were found on the second day of the simulations because semi-direct effects have more time to evolve.

Comparing the onlyMET with the VOLC model simulations revealed average vertical wind speed differences within ± 0.3 m/s for all levels when the whole period and all radiosonde observations were considered. While the model runs generally overestimated wind speeds by up to 2 m/s in the atmospheric boundary layer, better agreement was found for upper levels.

The simulated averaged temperature profiles agreed reasonably well with the observations at all levels/altitudes. At lower altitudes, the model runs differed from each other by about 0.4 °C with higher values for the onlyMET run. At higher altitudes the temperature values produced by the VOLC run can reach on average values up to 0.6 °C above those of the onlyMET run. The temperature at the lower levels showed that the model runs and observations agreed to within 1 °C on average. At altitudes below 960 hPa the VOLC run produced lower temperatures than the onlyMET run and was in better agreement with the observations.

Analysis of individual stations and time steps showed that for surface and lower atmospheric levels the VOLC run was in better agreement with the radiosonde observations for stations that were influenced by the presence of the volcanic ash cloud. We presented a case during which a temperature inversion was preserved in the VOLC run due to degreased incoming radiation caused by high aerosol concentrations aloft. In comparison the onlyMET run did not reproduce the temperature inversion apparent during day time.

It is worth mentioning some of the limiting factors of this study. The work presented in this paper included a range of different areas (volcanic eruptions, NWP, and air quality modeling), also subject to their own uncertainties. Not only are the emissions of the volcanic eruption quite complex, but also the contribution of other aerosol sources, e.g. desert dust emissions and anthropogenic contributions were estimated on best effort basis. Furthermore, the uncertainties of transport processes over large areas and the representation of the coupling between atmospheric aerosols and meteorological parameters in the model are complex processes. The relatively coarse grid used in our study for WRF-Chem of 12 km is also not always appropriate to compare gridded model outputs to point observations.

It was shown for selected cases that the coupled WRF-Chem model simulated a slightly improved atmospheric state in the presence of a volcanic cloud and highlighted that the current aerosol parameterization within WRF-Chem was both useful and provided an added value to “only meteorological” runs results compared to observational data.

Acknowledgments

This work has been supported by the BMWFW through funding of the VASCHBAER project (2015). This publication in part is the result of research sponsored by the Cooperative Institute for Alaska Research with funds from the National Oceanic and Atmospheric Administration under cooperative agreement NA13OAR4320056 with the University of Alaska. The authors would also like to thank numerous data providers: ECMWF for providing meteorological model data, TNO and EMEP for providing anthropogenic emissions, EEA, Meteo France and EMPA by providing air quality measurements, and the WMO's Global Telecommunication System (GTS), which allowed access to the meteorological ground measurements. The authors also acknowledge EARLINET for providing aerosol LIDAR profiles available from the EARLINET webpage. The radiosonde data was obtained from the University of Wyoming (http://weather.uwyo.edu/upperair/sounding.html). The multi-source analysis in chapter 4.3 was performed on a data management platform (http://vtpip.zamg.ac.at/) which was developed in the frame of the ESA funded projects TAMP (“Technology and Atmospheric Mission Platform”) and VEEDAM (“Virtual Exploitation Environment Demonstration for Atmospheric Missions”).

Appendix A. Supplementary data

Supplementary data to this article can be found online at https://doi.org/10.1016/j.atmosenv.2018.10.058.

References

Ackermann, I.J., Hass, H., Memmesheimer, M., Ebel, A., Binkowski, F.S., Shankar, U.M.A., 1998. Modal aerosol dynamics model for Europe: development and first applications. Atmos. Environ. 32 (17), 2981–2999.

Alapaty, K., Mathur, R., Pleim, J., Hogrefe, C., Rao, S.T., Ramaswamy, V., Galmarini, S., Schaap, M., Makar, P., Vautard, R., Baklanov, A., 2012. New directions: understanding interactions of air quality and climate change at regional scales. Atmos. Environ. 49, 419–421.

Arason, P., Petersen, G.N., Bjornsson, H., 2011. Observations of the altitude of the volcanic plume during the eruption of Eyjafjallajökull, April–May 2010. Earth Syst. Sci. Data 3 (1), 9–17.

Baklanov, A., Schlünzen, K., Suppan, P., Baldasano, J., Brunner, D., Aksoyoglu, S., Carmichael, G., Douros, J., Flemming, J., Forkel, R., Galmarini, S., 2014. Online coupled regional meteorology chemistry models in Europe: current status and prospects. Atmos. Chem. Phys. 14 (1), 317–398.

Bangert, M., Kottmeier, C., Vogel, B., Vogel, H., 2011. Regional scale effects of the aerosol cloud interaction simulated with an online coupled comprehensive chemistry model. Atmos. Chem. Phys. 11 (9), 4411–4423.

Baró, R., Palacios-Peña, L., Baklanov, A., Balzarini, A., Brunner, D., Forkel, R., Hirtl, M., Honzak, L., Pérez, J.L., Pirovano, G., San José, R., 2017. Regional effects of atmospheric aerosols on temperature: an evaluation of an ensemble of online coupled models. Atmos. Chem. Phys. 17 (15), 9677.

Brunner, D., Savage, N., Jorba, O., Eder, B., Giordano, L., Badia, A., Balzarini, A., Baró, R., Bianconi, R., Chemel, C., Curci, G., 2015. Comparative analysis of meteorological performance of coupled chemistry-meteorology models in the context of AQMEII phase 2. Atmos. Environ. 115, 470–498.

Charlson, R., Schwartz, S., Hales, J., Cess, R., Coakley, J., Hansen, J., Hofmann, D., 1992. Climate forcing by anthropogenic aerosols. Science 255 (5043), 423–430. Retrieved from. http://www.jstor.org/stable/2876009.

Chen, F., Dudhia, J., 2011. Coupling an advanced land surface–hydrology model with the Penn State–NCAR MM5 modeling system. Part I: model implementation and sensitivity. Mon. Weather Rev. 129 (4), 569–585.

Forkel, R., Balzarini, A., Baró, R., Bianconi, R., Curci, G., Jiménez-Guerrero, P., Hirtl, M., Honzak, L., Lorenz, C., Im, U., Pérez, J.L., 2015. Analysis of the WRF-Chem contributions to AQMEII phase2 with respect to aerosol radiative feedbacks on meteorology and pollutant distributions. Atmos. Environ. 115, 630–645.

Freitas, S.R., Longo, K.M., Alonso, M.F., Pirre, M., Marecal, V., Grell, G., Stockler, R., Mello, R.F., Sánchez Gácita, M., 2011. PREP-CHEM-SRC–1.0: a preprocessor of trace gas and aerosol emission fields for regional and global atmospheric chemistry models. Geosci. Model Dev. (GMD) 4 (2), 419–433.

Grell, G.A., Freitas, S.R., 2013. A scale and aerosol aware stochastic convective parameterization for weather and air quality modeling. Atmos. Chem. Phys. Discuss. 13 (9).

Grell, G.A., Peckham, S.E., Schmitz, R., McKeen, S.A., Frost, G., Skamarock, W.C., Eder, B., 2005. Fully coupled “online” chemistry within the WRF model. Atmos. Environ. 39 (37), 6957–6975.

Grell, G., Freitas, S.R., Stuefer, M., Fast, J., 2011. Inclusion of biomass burning in WRF-Chem: impact of wildfires on weather forecasts. Atmos. Chem. Phys. 11 (11), 5289.

Gudmundsson, M.T., Thordarson, T., Höskuldsson, Á., Larsen, G., Björnsson, H., Prata, F.J., Oddsson, B., Magnússon, E., Högnadóttir, T., Petersen, G.N., Hayward, C.L., 2012. Ash generation and distribution from the April-May 2010 eruption of Eyjafjallajökull. Iceland, Scientific reports 2, 572.

Guenther, C.C., 2006. Estimates of global terrestrial isoprene emissions using MEGAN (model of emissions of gases and aerosols from nature). Atmos. Chem. Phys. 6.

Hansen, J., Sato, M., Ruedy, R., 1997. Radiative forcing and climate response. J. Geophys. Res.: Atmosphere 102 (D6), 6831–6864.

Hong, S.Y., Noh, Y., Dudhia, J., 2006. A new vertical diffusion package with an explicit

treatment of entrainment processes. Mon. Weather Rev. 134 (9), 2318–2341.
Iacono, M.J., Delamere, J.S., Mlawer, E.J., Shephard, M.W., Clough, S.A., Collins, W.D., 2008. Radiative forcing by long-lived greenhouse gases: calculations with the AER radiative transfer models. J. Geophys. Res.: Atmosphere 113 (D13).
Jacobson, M.Z., Kaufman, Y.J., Rudich, Y., 2007. Examining feedbacks of aerosols to urban climate with a model that treats 3-D clouds with aerosol inclusions. J. Geophys. Res.: Atmosphere 112 (D24).
Kong, X., Forkel, R., Sokhi, R.S., Suppan, P., Baklanov, A., Gauss, M., Brunner, D., Barò, R., Balzarini, A., Chemel, C., Curci, G., 2015. Analysis of meteorology–chemistry interactions during air pollution episodes using online coupled models within AQMEII phase-2. Atmos. Environ. 115, 527–540.
Mastin, L.G., Guffanti, M., Servranckx, R., Webley, P., Barsotti, S., Dean, K., Durant, A., Ewert, J.W., Neri, A., Rose, W.I., Schneider, D., 2009. A multidisciplinary effort to assign realistic source parameters to models of volcanic ash-cloud transport and dispersion during eruptions. J. Volcanol. Geoth. Res. 186 (1), 10–21.
Mastin, L., Bonadonna, C., Folch, A., Stunder, B., Webley, P., Pavolonis, M., 2014. Eruption Data for Ash-cloud Model Validation. https://vhub.org/resources/2431.
Randel, W.J., Wu, F., Gaffen, D.J., 2000. Interannual variability of the tropical tropopause derived from radiosonde data and NCEP reanalyses. J. Geophys. Res.: Atmosphere 105 (D12), 15509–15523.
Reid, G.C., Gage, K.S., 1985. Interannual variations in the height of the tropical tropopause. J. Geophys. Res.: Atmosphere 90 (D3), 5629–5635.
San José, R., Pérez, J.L., Balzarini, A., Baró, R., Curci, G., Forkel, R., Galmarini, S., Grell, G., Hirtl, M., Honzak, L., Im, U., 2015. Sensitivity of feedback effects in CBMZ/MOSAIC chemical mechanism. Atmos. Environ. 115, 646–656.
Santer, B.D., Sausen, R., Wigley, T.M.L., Boyle, J.S., AchutaRao, K., Doutriaux, C., Hansen, J.E., Meehl, G.A., Roeckner, E., Ruedy, R., Schmidt, G., 2003a. Behavior of tropopause height and atmospheric temperature in models, reanalyses, and observations: decadal changes. J. Geophys. Res.: Atmosphere 108 (D1).
Santer, B.D., Wehner, M.F., Wigley, T.M.L., Sausen, R., Meehl, G.A., Taylor, K.E., Ammann, C., Arblaster, J., Washington, W.M., Boyle, J.S., Brüggemann, W., 2003b. Contributions of anthropogenic and natural forcing to recent tropopause height changes. Science (Washington, D.C.) 301 (5632), 479–483.
Schaefer, K., Thomas, W., Peters, A., Ries, L., Obleitner, F., Schnelle-Kreis, J., Birmili, W., Diemer, J., Fricke, W., Junkermann, W., Pitz, M., 2011. Influences of the 2010 Eyjafjallajokull volcanic plume on air quality in the northern Alpine region. Atmos. Chem. Phys. 11 (16), 8555.
Schell, B., Ackermann, I.J., Hass, H., Binkowski, F.S., Ebel, A., 2001. Modeling the formation of secondary organic aerosol within a comprehensive air quality model system. J. Geophys. Res.: Atmosphere 106 (D22), 28275–28293.
Seity, Y., Brousseau, P., Malardel, S., Hello, G., Bénard, P., Bouttier, F., Lac, C., Masson, V., 2011. The AROME-France convective-scale operational model. Mon. Weather Rev. 139 (3), 976–991.
Solomos, S., Kallos, G., Kushta, J., Astitha, M., Tremback, C., Nenes, A., Levin, Z., 2011. An integrated modeling study on the effects of mineral dust and sea salt particles on clouds and precipitation. Atmos. Chem. Phys. 11 (2), 873–892.
Stockwell, W.R., Middleton, P., Chang, J.S., Tang, X., 1990. The second generation regional acid deposition model chemical mechanism for regional air quality modeling. J. Geophys. Res.: Atmosphere 95 (D10), 16343–16367.
Stuefer, M., Freitas, S.R., Grell, G., Webley, P., Peckham, S., McKeen, S.A., 2012. Inclusion of Ash and SO2 emissions from volcanic eruptions in WRF-CHEM: development and some applications. Geosci. Model Dev. Discuss. (GMDD) 5 (3), 2571–2597.
Thordarson, T., Self, S., 2003. Atmospheric and environmental effects of the 1783–1784 Laki eruption: a review and reassessment. J. Geophys. Res.: Atmosphere 108 (D1).
Twomey, S., 1977. The influence of pollution on the shortwave albedo of clouds. J. Atmos. Sci. 34 (7), 1149–1152.
Vestreng, V., Rigler, E., Adams, M., Kindbom, K., Pacyna, J.M., Denier van der Gon, H., Reis, S., Travnikov, O., 2006. Inventory Review 2006, Emission Data Reported to LRTAP and NEC Directive, Stage 1, 2 and 3 Review and Evaluation of Inventories of HM and POPs. EMEP/MSC-W Technical Report 1/2006. Norwegian Meteorological Institute, Oslo ISSN 1504–6179. http://www.emep.int/publ/reports/2006/emep technical 1 2006.pdf.
Visschedijk, A.J.H., Zandveld, P.Y.J., Denier Van Der Gon, H.A.C., 2007. A High Resolution Gridded European Emission Database for the EU Integrated Project GEMS, TNO. TNO-report, Apeldoorn, Netherlands.
Webley, P.W., Steensen, T., Stuefer, M., Grell, G., Freitas, S., Pavolonis, M., 2012. Analyzing the Eyjafjallajökull 2010 eruption using satellite remote sensing, lidar and WRF-Chem dispersion and tracking model. J. Geophys. Res.: Atmosphere 117 (D20).
Zhang, B., Wang, Y., Hao, J., 2015. Simulating aerosol–radiation–cloud feedbacks on meteorology and air quality over eastern China under severe haze conditions in winter. Atmos. Chem. Phys. 15 (5), 2387–2404.
Zhang, Y., 2008. Online-coupled meteorology and chemistry models: history, current status, and outlook. Atmos. Chem. Phys. 8 (11), 2895–2932.
Zhang, Y., Dubey, M.K., Olsen, S.C., Zheng, J., Zhang, R., 2009. Comparisons of WRF/Chem simulations in Mexico City with ground-based RAMA measurements during the 2006-MILAGRO. Atmos. Chem. Phys. 9 (11), 3777–3798.